

FEM Analysis of Micromachined Flow Sensors with Wheatstone Bridge Read-out

A. Talić¹, S. Čerimović¹, Franz Kohl¹, Roman Beigelbeck¹, F. Keplinger², and J. Schalko^{1,2}

ABSTRACT:

We performed FEM simulations of a micromachined flow sensor featuring four germanium thermistors embedded in a silicon membrane. The thermistors are connected to form a Wheatstone bridge, which is supplied by a constant current. In operational mode, the heated membrane is cooled by any passing flow and the local cooling rate depends on the flow velocity. Based on this sensor concept, we performed steady flow and flow step (transient) simulations. As output quantities, we analyze the voltage across the bridge U_B as well as the voltage at the bridge supply terminals U_{SUP} . The simulation results demonstrate the feasibility of the new concept and suggest that high flow sensitivities and fast response times in combination with extremely low power consumption can be accomplished.

ACKNOWLEDGMENT:

We greatly acknowledge partial support of this work by the Austrian Science Fund (FWF, research grant L234-N07), the European Community (EC), and the country of Lower Austria (NÖ).



COOPERATION:



Introduction

Commonly used micromachined calorimetric flow sensors feature heat source(s) and spatially separated temperature sensors. Contrary to the standard layout with a thin-film heating resistor, we utilize four germanium thermistors embedded in the silicon nitride membrane. These thermistors serve as heat sources as well as temperature sensors and are connected to form a Wheatstone bridge.

Modelling and Simulation

The time dependent FE analysis was based on the schematic cross section shown in Fig. 1. The employed heat transport model includes conduction and convection, whereas radiative heat transfer and effects of natural convection were neglected.

The sensor model comprises two air domains. Convective heat transfer is only considered in the upper one. The fluid velocity in x -direction is imposed as parabolic function with respect to the y -coordinate implying the non-slip boundary condition at the top and bottom of the flow channel walls. The flow is assumed to be laminar and is parallel to the sensor membrane. The boundary condition at the outlet of the flow compartment is implemented as convective flux, the remaining parts of the model circumference were kept at the ambient temperature ($T_{amb}=21^\circ\text{C}$). The electrical thermistor resistance is modelled as

$$R_{th,i}(\vartheta) = R_{th,0} \cdot e^{\alpha\vartheta_i}, \quad i = 1 \dots 4,$$

where $\alpha = -0.0179 / ^\circ\text{C}$ is the temperature coefficient of resistivity and $R_{th,0} = 200 \text{ k}\Omega$ the thermistor resistance at $\vartheta_i = 0^\circ\text{C}$. The thermistor excess temperatures ϑ_i were calculated through a subdomain integration of the variable T over each thermistor area. Figure 2 visualizes the simulated temperature field distribution for $v_{in} = 10 \text{ m/s}$.

The density of the dissipated power in the thermistor equals

$$Q_i = I_{th,i}^2 R_{th,i}(\vartheta_i) / V, \quad i = 1 \dots 4,$$

and depends indirectly on ϑ_i due to the thermistor effect. V specifies the thermistor volume and $I_{th,i}$ is the thermistor current:

$$I_{th,1} = I_{th,2} = I_{SUP} \frac{R_{th,3} + R_{th,4}}{R_{th,1} + R_{th,2} + R_{th,3} + R_{th,4}}, \quad I_{th,3} = I_{th,4} = I_{SUP} \frac{R_{th,1} + R_{th,2}}{R_{th,1} + R_{th,2} + R_{th,3} + R_{th,4}},$$

where $I_{SUP} = 50 \mu\text{A}$ denotes the constant bridge supply current. All thermistor temperatures are influenced by convective heat transfer on the one hand and the power dissipation Q_i on the other hand, which in turn depends on the temperature. Starting from the initial temperature, the values $R_{th,i}$, $I_{th,i}$, and hence Q_i are computed. The first value of Q_i is imposed and the thermistor temperatures are calculated anew. In subsequent computational steps, Q_i is updated until a steady-state is reached.

Results and Discussion

The voltage across the bridge U_B and at the bridge supply terminals U_{SUP} depends on the thermistor resistance values and hence on the flow velocity

$$U_B = I_{SUP} \frac{R_{th,2}R_{th,3} - R_{th,1}R_{th,4}}{R_{th,1} + R_{th,2} + R_{th,3} + R_{th,4}}, \quad U_{SUP} = I_{SUP} \frac{(R_{th,1} + R_{th,2})(R_{th,3} + R_{th,4})}{R_{th,1} + R_{th,2} + R_{th,3} + R_{th,4}}.$$

With increasing flow, the thermistors next to flow inlet ($R_{th,2}$ and $R_{th,3}$) are cooled down more efficient than the thermistors near the flow outlet ($R_{th,1}$ and $R_{th,4}$). Figure 3 shows the dependence of thermistor temperatures ϑ_i on the average flow velocity.

Evaluating the bridge voltage U_B for steady flow, an excellent sensitivity for flow velocities below 2 m/s was achieved. For higher velocities, however, the output characteristic becomes ambiguous. In contrast, the supply voltage U_{SUP} offers a wider measurement range but moderate sensitivity at lower velocities (Fig. 3b). To compute the transient behaviour in response to a flow step (Fig. 4), the stationary simulation results for $v_{in} = 0 \text{ m/s}$ (no flow) were used as initial state. For both functional modes, the related rise time depends on the height of the flow step. In case of U_B , only a few milliseconds are observed.

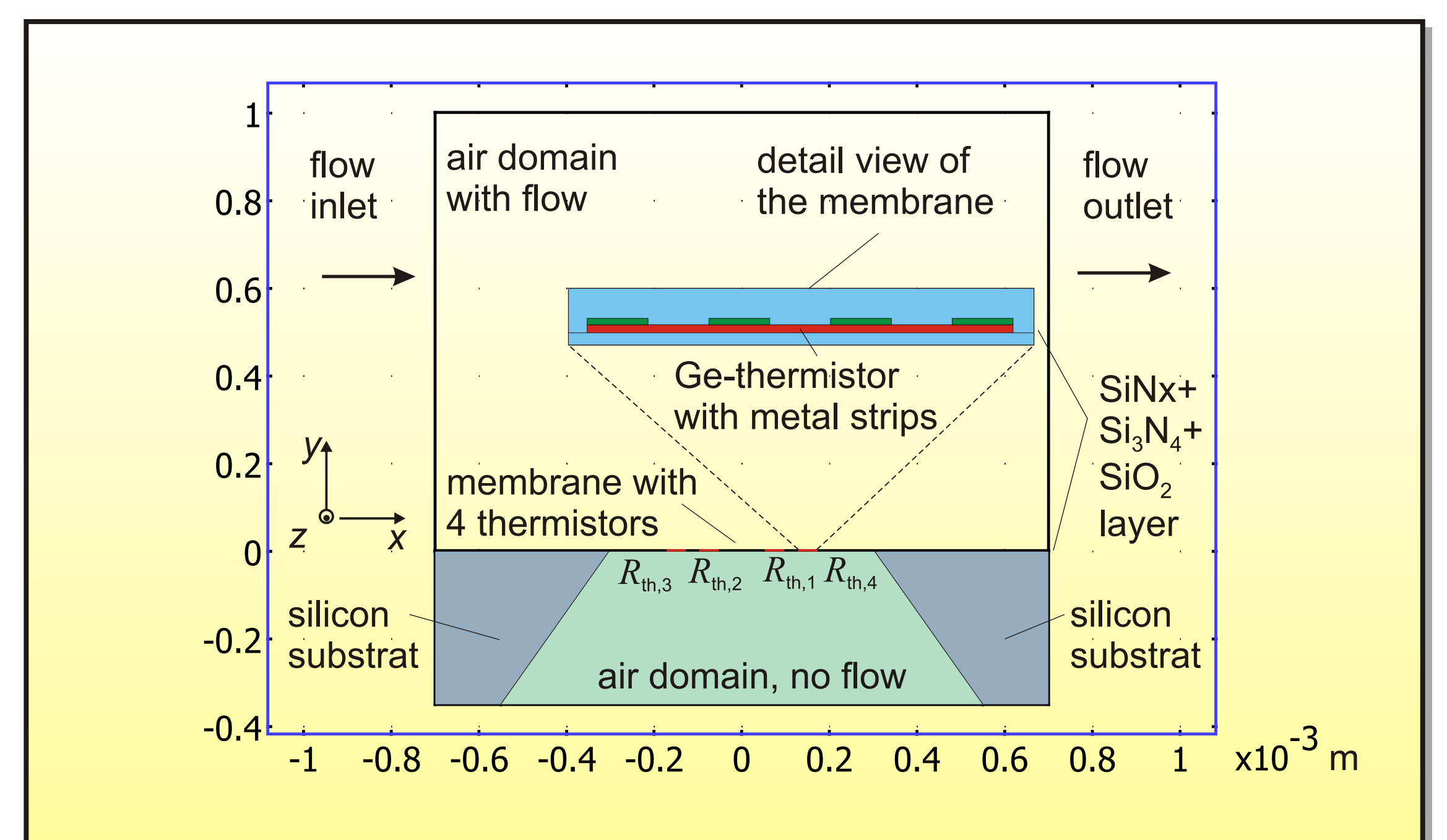


Fig. 1: Simplified 2D-model comprising four membrane thermistors. The sensor membrane consists of the SiO_2 and Si_3N_4 wafer coating, and the passivation layer SiN_x , featuring 150 nm, 200 nm, and 1250 nm thickness, respectively. Each of thermistors consists of a 220 nm thick germanium film, which is contacted by four metal strips (180 nm thick). The sensor membrane features an overall thickness of about 1.6 μm and is supported by a micromachined silicon frame (350 μm thick).

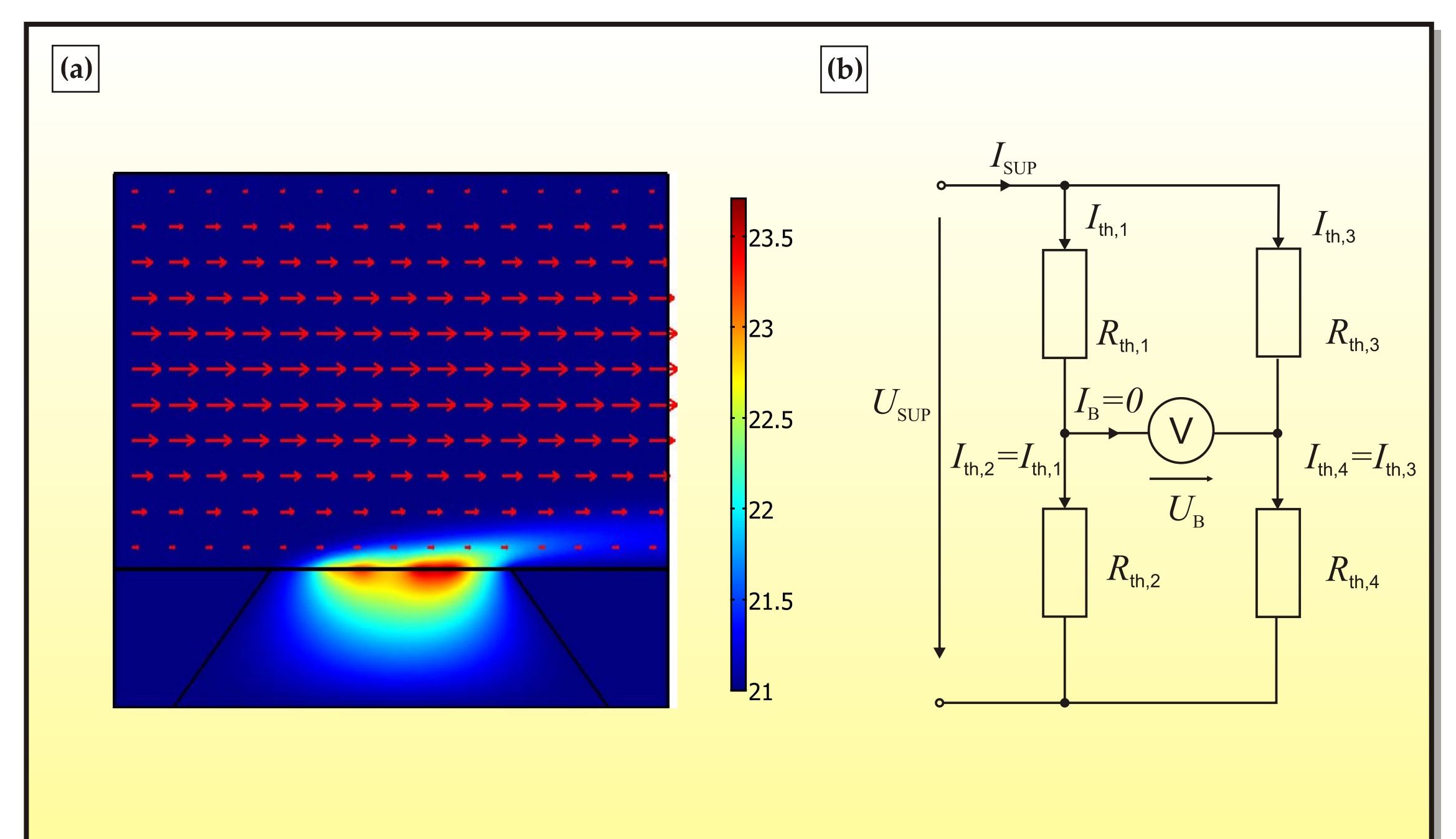


Fig. 2: Simulated temperature distribution at the symmetry plane of the sensor for an average flow velocity of 10 m/s (parabolic flow profile in the channel). A two dimensional (2D) model seems reasonable since all thin-film components on the membrane exhibit a large extension perpendicular to the flow direction. The sensor device is mounted flush with the wall of a flow channel (height 1 mm).

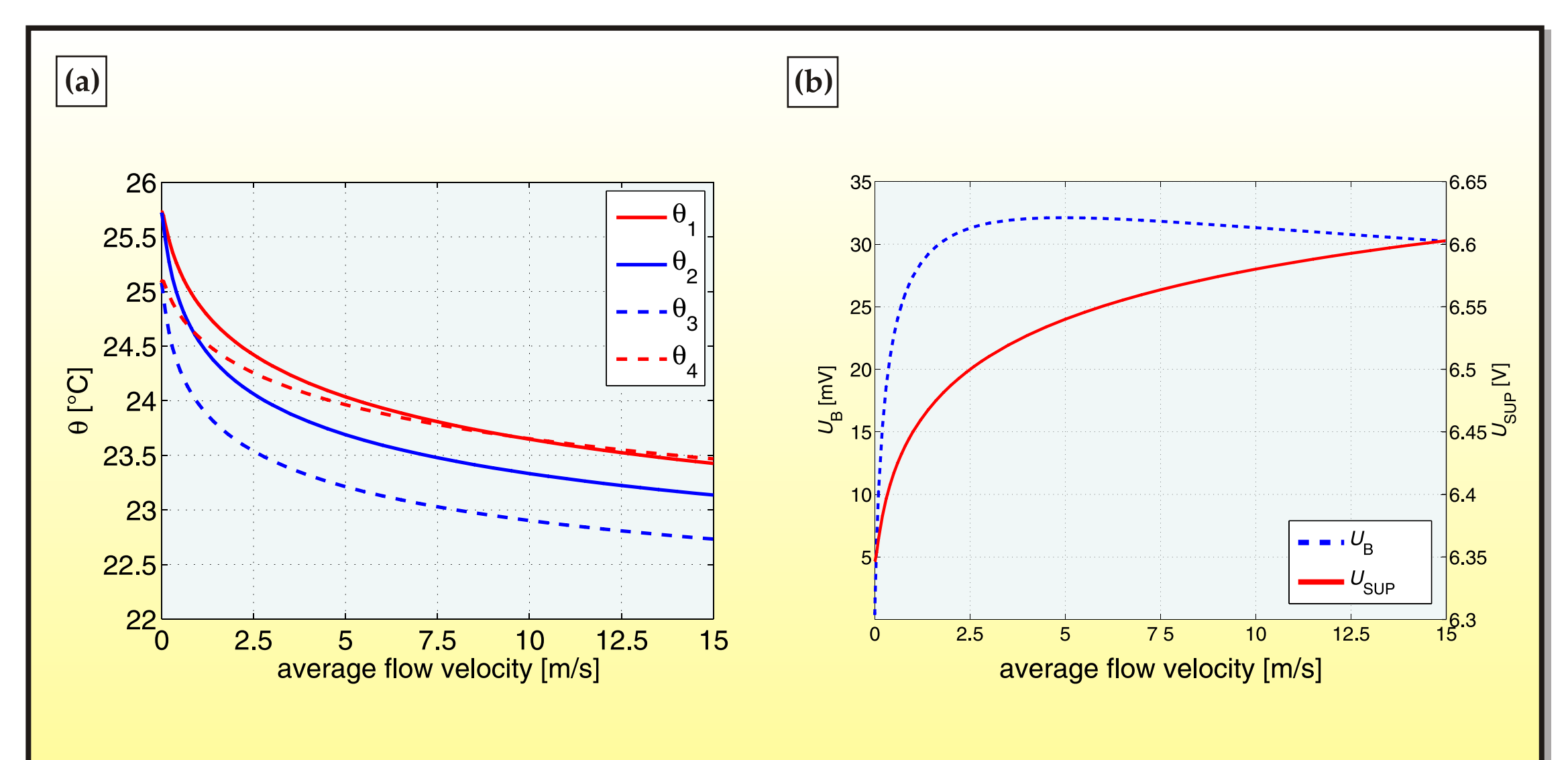


Fig. 3: (a) Thermistor temperatures ϑ_i over the average flow velocity. By connecting the thermistors as shown in Fig. 1, one achieves the best possible sensitivity. (b) Output characteristics of the flow sensor using the voltage across the bridge U_B and the voltage at the bridge supply terminals U_{SUP} as an output quantity.

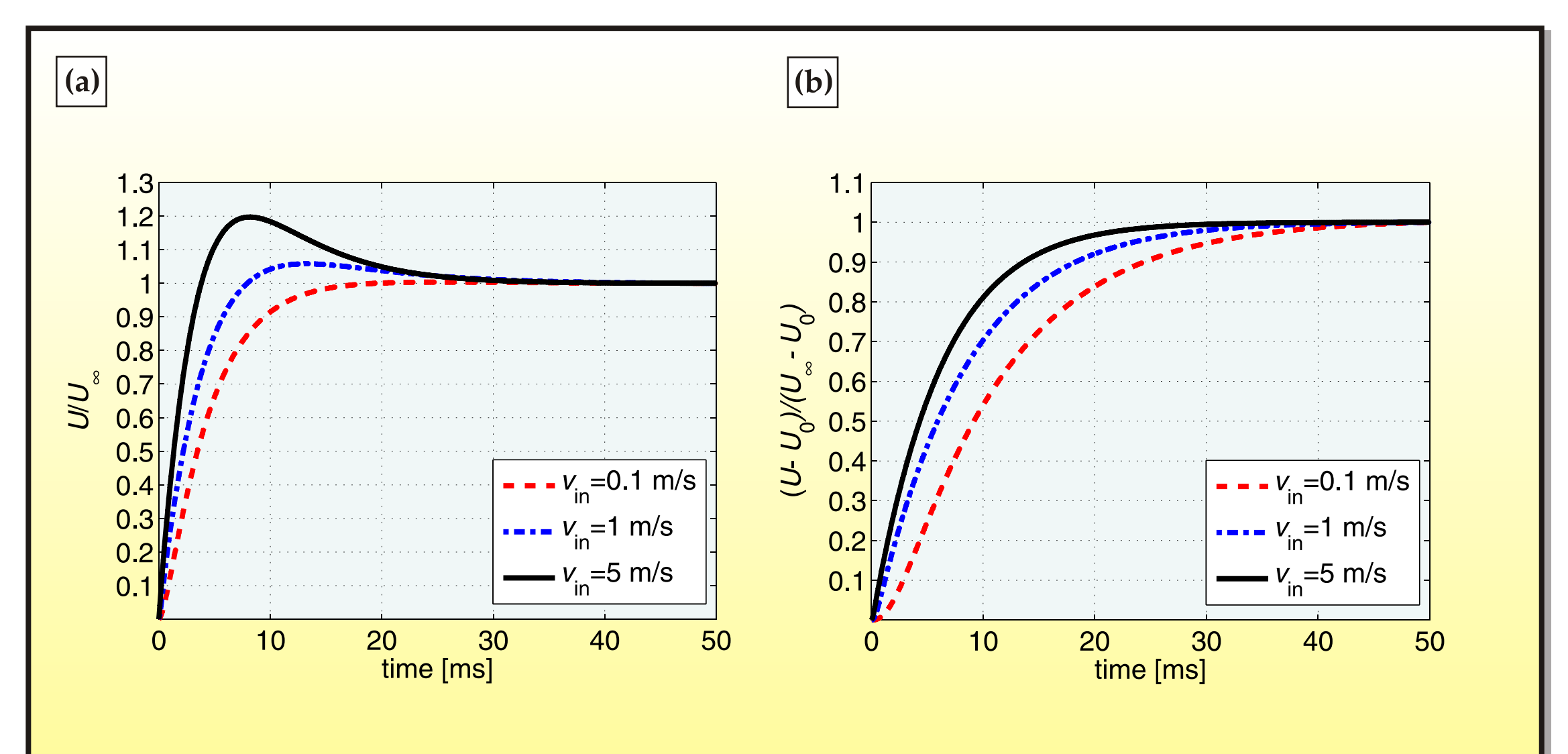


Fig. 4: Relative flow step response of (a) the bridge voltage U_B and of (b) the bridge supply terminals voltage U_{SUP} for different heights of the flow step. U_0 is the initial value, while U_∞ denotes the final value.

¹ Research Unit for Integrated Sensor Systems, Austrian Academy of Sciences
Viktor Kaplan Straße 2, A-2700 Wiener Neustadt, Austria
Phone: +43 2622 23420-21 ; Fax: +43 2622 23420-99
{Almir.Talic, Samir.Cerimovic, Franz.Kohl, Roman.Beigelbeck}@OEAW.ac.at
http://www.oew.ac.at/fiss

² Institute of Sensor and Actuator Systems, Vienna University of Technology
Gusshausstraße 27-29, A-1040 Vienna, Austria
Phone: +43 | 58801-36662 ; Fax: +43 | 58801-36699
{Franz.Keplinger, Johannes.Schalko}@TUWien.ac.at
http://www.isas.tuwien.ac.at